Chapter 2
Bifurcations and Chaos in Dynamical Systems

Complex system theory deals with dynamical systems containing often a large number of variables. It extends dynamical system theory, which deals with dynamical systems containing a few variables. A good understanding of dynamical systems theory is therefore a prerequisite when studying complex systems.

In this chapter we introduce important concepts, like attractors and Lyapunov exponents, bifurcations, and deterministic chaos from the realm of dynamical system theory. An introduction to catastrophe theory will be provided together with the notion of colliding attractors and global bifurcations.

Most of the chapter will be devoted to ordinary differential equations and maps, the traditional focus of dynamical system theory, venturing however towards the end into the intricacies of time-delayed dynamical systems.

2.1 Basic Concepts of Dynamical Systems Theory

Dynamical systems theory deals with the properties of coupled differential equations, determining the time evolution of a few, typically a handful of variables. Many interesting concepts have been developed and we will present a short overview covering the most important phenomena.

Fixpoints and Limit Cycles We start by discussing an elementary nonlinear rotator, just to illustrate some procedures that are typical for dynamical systems theory. We consider a two-dimensional system $\mathbf{x} = (x, y)$. Using polar coordinates

$$x(t) = r(t)\cos(\varphi(t)), \qquad y(t) = r(t)\sin(\varphi(t)) \ , \tag{2.1}$$

we assume that the following non-linear differential equations:

$$\dot{r} = (\Gamma - r^2)\, r, \qquad \dot{\varphi} = \omega \tag{2.2}$$

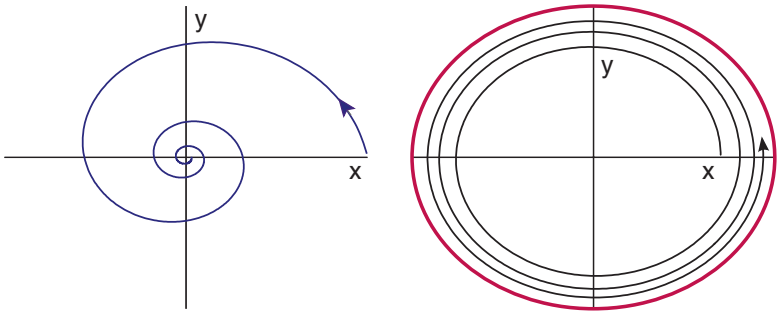

Fig. 2.1 The solution of the non-linear rotator, compare Eqs. (2.1) and (2.2), for $\Gamma < 0$ (left, with a stable fixpoint) and $\Gamma > 0$ (right, with a limit cycle).

govern the dynamical behavior. The typical orbits $(x(t), y(t))$ are illustrated in Fig. 2.1. The limiting behavior of Eq. (2.2) is

$$\lim_{t\to\infty} \begin{bmatrix} x(t) \\ y(t) \end{bmatrix} = \begin{cases} \begin{bmatrix} 0 \\ 0 \end{bmatrix} & \Gamma < 0 \\ \begin{bmatrix} r_c \cos(\omega t) \\ r_c \sin(\omega t) \end{bmatrix} & r_c^2 = \Gamma > 0 \end{cases} . \tag{2.3}$$

In the first case, $\Gamma < 0$, we have a stable fixpoint $\mathbf{x}_0^* = (0, 0)$ to which the trajectories are attracted. In the second case, $\Gamma > 0$, the dynamics approaches a limit cycle.

> Bifurcation. The long-term limiting behavior of a dynamical system described by a set of parameterized differential equations may change qualitatively as a function of an external parameter. The resulting change in terms of fixpoints, limit cycles and/or chaotic attractors constitutes a bifurcation.

The dynamical system (2.1) and (2.2) shows a bifurcation at $\Gamma = 0$, a fixpoint turns into a limit cycle at $\Gamma = 0$. One denotes this specific type of bifurcation as a "Hopf bifurcation"; we will discuss bifurcation theory in greater detail in Sect. 2.2.

Stability of Fixpoints The dynamics of orbits close to a fixpoint or a limiting orbit determines its stability.

> Stability Condition. A fixpoint is stable (unstable) if nearby orbits are attracted (repelled) by the fixpoint, and metastable if the distance does not change.

An illustration is given in Fig. 2.2. The stability of fixpoints is closely related to their Lyapunov exponents, as discussed in Sect. 2.4.

One can examine the stability of a fixpoint $\mathbf{x}^*$ by linearizing the equation of motions for $\mathbf{x} \approx \mathbf{x}^*$. For the fixpoint $r^* = 0$ of Eq. (2.2) we find

$$\dot{r} = \left(\Gamma - r^2\right) r \approx \Gamma r \qquad r \ll 1 \ ,$$

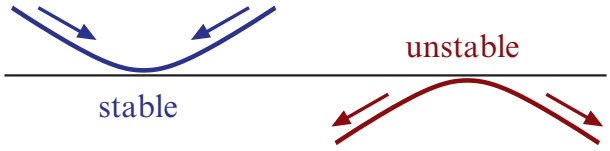

Fig. 2.2 A fixpoint is stable (unstable) when orbits are attracted (repelled).

and $r(t)$ decreases (increases) for $\Gamma < 0$ ($\Gamma > 0$). For a d-dimensional system $\mathbf{x} = (x_1, \ldots, x_d)$ the stability of a fixpoint $\mathbf{x}^*$ is determined by calculating the d eigenvalues of the linearized equations of motion. The system is stable if all eigenvalues are negative and unstable if at least one eigenvalue is positive.

First-Order Differential Equations Let us consider the third-order differential equation

$$\frac{d^3}{\mathrm{d}t^3}x(t) = f(x, \dot{x}, \ddot{x}) \ . \tag{2.4}$$

Using

$$x_1(t) = x(t), \qquad x_2(t) = \dot{x}(t), \qquad x_3(t) = \ddot{x}(t) \ , \tag{2.5}$$

we can rewrite (2.4) as a first-order differential equation:

$$\frac{\mathrm{d}}{\mathrm{d}t}\begin{bmatrix} x_1 \\ x_2 \\ x_3 \end{bmatrix} = \begin{bmatrix} x_2 \\ x_3 \\ f(x_1, x_2, x_3) \end{bmatrix} \ .$$

Autonomous Systems It is then generally true that one can reduce any set of coupled differential equations to a set of first-order differential equations by introducing an appropriate number of additional variables. We therefore consider in the following only first-order, ordinary differential equations such as

$$\frac{\mathrm{d}\mathbf{x}(t)}{\mathrm{d}t} = \mathbf{f}(\mathbf{x}(t)), \qquad \mathbf{x}, \mathbf{f} \in \mathbb{R}^d, \qquad t \in [-\infty, +\infty] \ , \tag{2.6}$$

when time is continuous, or, equivalently, maps such as

$$\mathbf{x}(t+1) = \mathbf{g}(\mathbf{x}(t)), \qquad \mathbf{x}, \mathbf{g} \in \mathbb{R}^d, \qquad t = 0, 1, 2, \ldots \ , \tag{2.7}$$

when time is discrete. Together with the time evolution equation one has to set the initial condition $\mathbf{x}_0 = \mathbf{x}(t_0)$. An evolution equation of type Eq. (2.6) is denoted "autonomous", since it does not contain an explicit time dependence. A system of type $\dot{\mathbf{x}} = \mathbf{f}(t, \mathbf{x})$ is dubbed "non-autonomous".

PHASE SPACE. One denotes by "phase space" the space spanned by all allowed values of the variables entering the set of first-order differential equations defining the dynamical system.

The phase space depends on the representation. For a two-dimensional system (x, y) the phase space is just $\mathbb{R}^2$, but in the polar coordinates Eq. (2.1) it is

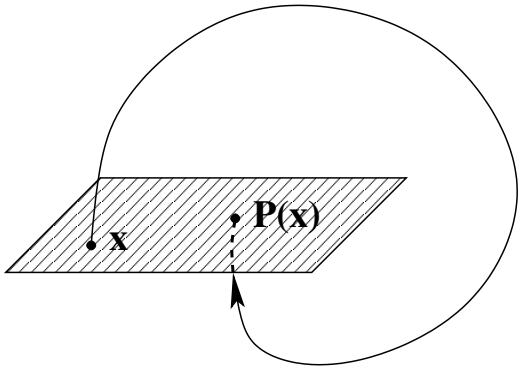

Fig. 2.3 The Poincaré map $\mathbf{x} \to \mathbf{P}(\mathbf{x})$, mapping an intersection $\mathbf{x}$ of the trajectory with a hyperplane (indicated by *shaded region*) to the consecutive intersection $\mathbf{P}(\mathbf{x})$.

$$\left\{ (r, \varphi) \,\middle|\, r \in [0, \infty],\, \varphi \in [0, 2\pi[\right\} .$$

Orbits and Trajectories A particular solution $\mathbf{x}(t)$ of the dynamical system Eq. (2.6) can be visualized as a "trajectory", also denoted "orbit", in phase space. Any orbit is uniquely determined by the set of "initial conditions", $\mathbf{x}(0) \equiv \mathbf{x}_0$, since we are dealing with first-order differential equations.

Poincaré Map It is in general difficult to illustrate graphically the motion of $\mathbf{x}(t)$ in d dimensions. Our retina, as well as our print media, are two-dimensional and it is therefore convenient to consider a plane Σ in $\mathbb{R}^d$ and the points $\mathbf{x}^{(i)}$ of the intersection of an orbit γ with Σ, see Fig. 2.3.

For the purpose of illustration let us consider the plane

$$\Sigma = \{ (x_1, x_2, 0, \ldots, 0) \,|\, x_1, x_2 \in \mathbb{R} \}$$

and the sequence of intersections (see Fig. 2.3)

$$\mathbf{x}^{(i)} = (x_1^{(i)}, x_2^{(i)}, 0, \ldots, 0), \qquad (i = 1, 2, \ldots)$$

which define the "Poincaré map"

$$\mathbf{P} : \ \mathbf{x}^{(i)} \ \mapsto \ \mathbf{x}^{(i+1)} \ . \tag{2.8}$$

The Poincaré map is a discrete map, compare (2.7), which can be constructed for continuous-time dynamical systems like Eq. (2.6). The Poincaré map is very useful, since we can print and analyze it directly. A periodic orbit, to give an example, would show up in the Poincaré map as the identity mapping.

Constants of Motion and Ergodicity We mention here a few general concepts from the theory of dynamical systems.

– Constant of Motion: A function $F(\mathbf{x})$ on phase space $\mathbf{x} = (x_1, \ldots, x_d)$ is called a "constant of motion" or a "conserved quantity" if it is conserved under the time evolution of the dynamical system, i.e. when

$$\frac{\mathrm{d}}{\mathrm{d}t} F(\mathbf{x}(t)) = \sum_{i=1}^{d} \left(\frac{\partial}{\partial x_i} F(\mathbf{x}) \right) \dot{x}_i(t) \equiv 0$$

holds for all times t. In many mechanical systems the energy is a conserved quantity.
– Ergodicity : A dynamical system in which orbits come arbitrarily close to any allowed point in the phase space, irrespective of the initial condition, is called ergodic.
All conserving systems of classical mechanics, obeying Hamiltonian dynamics, are ergodic. The ergodicity of a mechanical system is closely related to "Liouville's theorem", which will be discussed in Sect. 3.1.1 of Chap. 3, "Dissipation, Noise and Adaptive Systems".
Ergodicity holds only modulo conserved quantities, as is the case for the energy in many mechanical systems. Then, only points in the phase space having the same energy as the trajectory considered are approached arbitrarily close.
– Attractors: A bounded region in phase space to which orbits with certain initial conditions come arbitrarily close is called an attractor.
Attractors can be isolated points (fixpoints), limit cycles or more complex objects.
– Basin of Attraction: The set of initial conditions that leads to orbits approaching a certain attractor arbitrarily closely is called the basin of attraction.

It is clear that ergodicity and attractors are mutually exclusive: An ergodic system cannot have attractors and a dynamical system with one or more attractors cannot be ergodic.

Mechanical Systems and Integrability A dynamical system of type

$$\ddot{x}_i = f_i(\boldsymbol{x}, \dot{\boldsymbol{x}}), \qquad i = 1, \ldots, f$$

is denoted a "mechanical system" since all equations of motion in classical mechanics are of this form, e.g. Newton's law. f is called the degree of freedom and a mechanical system can be written as a set of coupled first-order differential equations with $2f$ variables

$$(x_1 \ldots x_f, v_1 \ldots v_f), \qquad v_i = \dot{x}_i, \qquad i = 1, \ldots, f$$

constituting the phase space, with $\mathbf{v} = (v_1, \ldots, v_f)$ being denoted the generalized velocity. A mechanical system is "integrable" if there are $\alpha = 1, \ldots, f$ independent constants of motion $F_\alpha(\boldsymbol{x}, \dot{\boldsymbol{x}})$, with

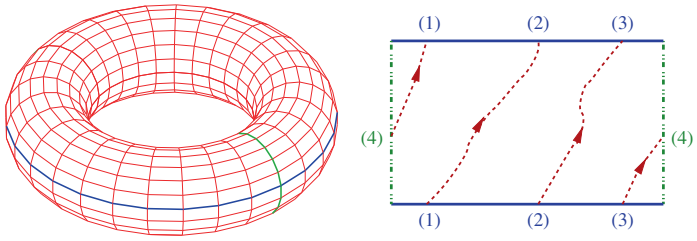

Fig. 2.4 Left: The KAM-torus can be cut along two lines (vertical/horizontal) and unfolded. **Right:** A closed orbit on the unfolded torus with $\omega_1/\omega_2 = 3/1$. The numbers indicate points that coincide after refolding (periodic boundary conditions).

$$\frac{d}{\mathrm{d}t} F_\alpha(\boldsymbol{x}, \dot{\boldsymbol{x}}) = 0, \qquad \alpha = 1, \ldots, f \ .$$

The motion in the $2f$-dimensional phase space $(x_1 \ldots x_f, v_1 \ldots v_f)$ is then restricted to an f-dimensional subspace, which is an f-dimensional torus, see Fig. 2.4.

An example of an integrable mechanical system is the Kepler problem, viz the motion of the earth around the sun. Integrable systems, however, are very rare, but they constitute important reference points for the understanding of more general dynamical systems. A classical example of a non-integrable mechanical system is the three-body problem, viz the combined motion of earth, moon and sun around each other.

KAM Theorem Kolmogorov, Arnold and Moser (KAM) have examined the question of what happens to an integrable system when it is perturbed. Let us consider a two-dimensional torus, as illustrated in Fig. 2.4. The orbit wraps around the torus with frequencies ω_1 and ω_2, respectively. A key quantity is the ratio of revolution frequencies ω_1/ω_2; it might be rational or irrational.

We remember that any irrational number r may be approximated with arbitrary accuracy by a sequence of quotients

$$\frac{m_1}{s_1}, \ \frac{m_2}{s_2}, \ \frac{m_3}{s_3}, \ \ldots \qquad\qquad s_1 < s_2 < s_3 < \ldots$$

with ever larger denominators s_i. A number r is "very irrational" when it is difficult to approximate r by such a series of rational numbers, viz when very large denominators s_i are needed to achieve a certain given accuracy $|r - m/s|$.

The KAM theorem states that orbits with rational ratios of revolution frequencies ω_1/ω_2 are the most unstable under a perturbation of an integrable system and that tori are most stable when this ratio is very irrational.

Gaps in the Saturn Rings A spectacular example of the instability of rational KAM-tori are the gaps in the rings of the planet Saturn.

The time a particle orbiting in Cassini's gap (between the A-ring and the B-ring, $r = 118{,}000\,\mathrm{km}$) would need around Saturn is exactly half the time the "shepherd-moon" Mimas needs to orbit Saturn. The quotient of the revolving frequencies is 2:1. Any particle orbiting in Cassini's gap is therefore unstable against the perturbation caused by Mimas and it is consequently thrown out of its orbit.

2.2 Fixpoints, Bifurcations and Stability

We start by considering the stability of fixpoint x^* of a one-dimensional dynamical system

$$\dot{x} = f(x), \qquad f(x^*) = 0\ . \tag{2.9}$$

"Invariant manifolds" are sets of phase space that that are invariant under the dynamical flow, a subject touched upon further in in Sect. 3.1.4 of Chap. 3, "Dissipation, Noise and Adaptive Systems". Per difinition, a fixpoint is an invariant manifold.

Fixpoints are the only possible invariant manifolds for $d = 1$ dimension, in two dimensions fixpoints and limiting cycles are possible and more complicated objects, such as strange attractors, become possible in three and higher dimensions.

Stability of Fixpoints The stability of a fixpoint is determined by the direction of the flow close to it, which can be determined by linearizing the time evolution equation $\dot{x} = f(x)$ around the fixpoint x^*,

$$\frac{d}{dt}(x - x^*) = \dot{x} \approx\ f(x^*)\ +\ f'(x^*)(x - x^*)\ +\ \dots\ , \tag{2.10}$$

where $f'()$ denotes the first derivative. We rewrite (2.10) as

$$\frac{d}{dt}\Delta x = f'(x^*)\,\Delta x, \qquad \Delta x = x - x^*$$

where we have neglected terms of order $(x - x^*)^2$ and higher and where we have made use of the fixpoint condition $f(x^*) = 0$. This equation has the solution

$$\Delta x(t) = \Delta x(0)\,\mathrm{e}^{tf'(x^*)}\ \rightarrow\ \begin{cases} \infty & f'(x^*) > 0 \\ 0 & f'(x^*) < 0 \end{cases}\ . \tag{2.11}$$

The perturbation Δx decreases/increases with time and the fixpoint x^* is hence stable/unstable for $f'(x^*) < 0$ and $f'(x^*) > 0$ respectively. For more than a single variable one has to find all eigenvalues of the linearized problem and the fixpoint is stable only when all eigenvalues are negative, as discussed more in depth in Sect. 2.2.1.

Lyapunov Exponents The flow of $\dot{x} = f(x)$ changes sign at the locus of the fixpoint x^*, compare Fig. 2.9.

LYAPUNOV EXPONENT. The time evolution close to a fixpoint x^* is generically exponential, $\sim \exp(\lambda t)$, and one denotes by $\lambda = f'(x^*)$ the Lyapunov exponent.

The Lyapunov exponent controls the sign change and the direction of the flow close to a fixpoint. Orbits are exponentially repelled/attracted for $\lambda > 0$ and for $\lambda < 0$ respectively.

Fixpoints of Discrete Maps For a discrete map of type

$$x(t+1) = g(x(t)), \qquad x^* = g(x^*) \tag{2.12}$$

the stability of a fixpoint x^* can be determined by an equivalent linear analysis,

$$x(t+1) = g(x(t)) \approx g(x^*) \; + \; g'(x^*)(x(t) - x^*) \; .$$

Using the fixpoint condition $g(x^*) = x^*$ we write above expression as

$$\Delta x(t+1) = x(t+1) - x^* = g'(x^*)\, \Delta x(t) \; ,$$

with the solution

$$\Delta x(t) = \Delta x(0) \left[g'(x^*)\right]^t, \qquad |\Delta x(t)| = |\Delta x(0)|\, \mathrm{e}^{\lambda t} \; . \tag{2.13}$$

The Lyapunov exponent

$$\lambda = \log |g'(x^*)| = \begin{cases} < 0 & \text{for} \quad |g'(x^*)| < 1 \\ > 0 & \text{for} \quad |g'(x^*)| > 1 \end{cases} \tag{2.14}$$

controls the stability of the fixpoint. Note the differences in the relation of the Lyapunov exponent λ to the derivatives $f'(x^*)$ and $g'(x^*)$ for differential equations and maps respectively, compare Eqs. (2.11) and (2.14).

2.2.1 Fixpoints Classification and Jacobian

We now consider a general d-dimensional dynamical system of type (2.6),

$$\frac{\mathrm{d}\mathbf{x}(t)}{\mathrm{d}t} = \mathbf{f}(\mathbf{x}(t)), \qquad \mathbf{x}, \mathbf{f} \in \mathbb{R}^d, \qquad \mathbf{f}(\mathbf{x}^*) = 0 \; , \tag{2.15}$$

having a fixpoint $\mathbf{x}^*$.

Jacobian and Lyapunov Exponents For a stability analysis of the fixpoint $\mathbf{x}^*$ one linearizes (2.15) around the fixpoint, using $x_i(t) \approx x_i^* + \delta x_i(t)$, with small $\delta x_i(t)$. One obtains

$$\frac{d\delta x_i}{dt} = \sum_j J_{ij}\,\delta x_j, \qquad J_{ij} = \left.\frac{\partial f_i(\mathbf{x})}{\partial x_j}\right|_{\mathbf{x}=\mathbf{x}^*} . \tag{2.16}$$

The matrix J_{ij} of all possible partial derivatives is called the "Jacobian" of the dynamical system (2.15). One then generalizes the definition of the Lyapunov exponent for one-dimensional systems, as given previously in Sect. 2.2.

LYAPUNOV SPECTRUM. The set of eigenvalues $\{\lambda_i\}$ of the Jacobian $i = 1, .., d$ is the spectrum characterizing the fixpoint $\mathbf{x}^*$.

Lyapunov exponents $\lambda_n = \lambda'_n + i\lambda''_n$ may have real λ'_n and imaginary λ''_n components and characterize the time evolution

$$\mathrm{e}^{\lambda_n t} = \mathrm{e}^{\lambda'_n t}\,\mathrm{e}^{i\lambda''_n t}$$

of infinitesimal perturbations around the fixpoint. A Lyapunov exponent λ_n is attracting/neutral/repelling when λ'_n is negative/zero/positive respectively.

Hyperbolic Fixpoints The flow is well defined in linear order when all $\lambda'_i \neq 0$. In this case the fixpoint is said to be "hyperbolic". For a non-hyperbolic fixpoint at least one of the Lyapunov exponents is neutral. All Lyapunov exponents are neutral for a vanishing Jacobian.

Pairwise Conjugate Exponents With $\lambda = \lambda' + i\lambda''$ also its conjugate $\lambda^* = \lambda' - i\lambda''$ in an eigenvalue of the Jacobian, which is a real matrix. λ and λ^* differ for $\lambda'' \neq 0$ and in this case there are two eigenvalues having the same real part λ'.

Classification of Fixpoints for $d = 2$ In Fig. 2.5 some example trajectories are shown for several fixpoints in $d = 2$ dimensions.

- Node: Both eigenvalues are real and have the same sign, which is negative/positive for a stable/unstable node.
- Saddle: Both eigenvalues are real and have opposite signs.
- Focus: The eigenvalues are complex conjugate to each other. The trajectories spiral in/out for negative/positive real parts.

Fixpoints in higher dimensions are characterized by the number of respective attracting/neutral/repelling eigenvalues of the Jacobian, which may be in turn either real or complex.

Stable and Unstable Manifolds For real eigenvalues $\lambda_n \neq 0$ of the Jacobian J, with eigenvectors $\mathbf{e}_n$ and a sign $s_n = \lambda_n/|\lambda_n|$, we can define via

$$\lim_{t \to -s_n \infty} \mathbf{x}_n(t) = \mathbf{x}^* + e^{t\lambda_n}\mathbf{e}_n, \qquad J\mathbf{e}_n = \lambda_n \mathbf{e}_n \ , \tag{2.17}$$

trajectories $\mathbf{x}_n(t)$ called "stable manifolds" (for $\lambda_n < 0$) and "unstable manifolds" (for $\lambda_n > 0$).

For a neutral Lyapunov exponent with $\lambda_n = 0$ one can define a "center manifold" which we will discuss in the context of catastrophe theory in

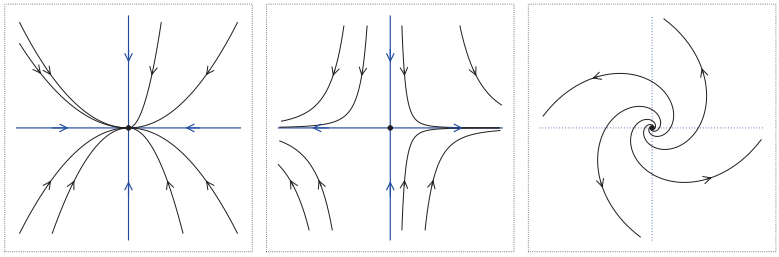

Fig. 2.5 Example trajectories for a stable node (left), with a ratio $\lambda_2/\lambda_1 = 2$, for a saddle (middle) with $\lambda_2/\lambda_1 = -3$ and for a unstable focus (right).

Sect. 2.3.1. The term "manifold" denotes in mathematics, loosely speaking, a smooth topological object.

Stable and unstable manifolds control the flow infinitesimal close to the fixpoint along the eigendirections of the Jacobian and may be continued to all positive and negative times t. Typical examples are illustrated in Figs. 2.5 and 2.6.

Heteroclinic orbits One speaks of a "heteroclinc orbit" when the unstable manifold of one fixpoint connects to the stable manifold of another fixpoint. As an example, we consider a two dimensional dynamical system defined by

$$\begin{aligned} \dot{x} &= 1 - x^2 \\ \dot{y} &= yx + \epsilon\left(1 - x^2\right)^2 \end{aligned} \qquad J(x^*) = \begin{pmatrix} -2x^* & 0 \\ 0 & x^* \end{pmatrix} \tag{2.18}$$

with the two saddles $\mathbf{x}^*_\pm = (x^*, 0)$, where $x^* = \pm 1$. The eigenvectors of the Jacobian $J(x^*)$ are aligned with the x and the y axis respectively, for all values of the control parameter ϵ.

The flow diagram is illustrated in Fig. 2.6, it is invariant when inverting both $x \leftrightarrow (-x)$ and $y \leftrightarrow (-y)$. The system contains additionally the $y = 0$ axis as a mirror line for a vanishing $\epsilon = 0$ and there is a heteroclinic orbit connecting the unstable manifold of $\mathbf{x}^*_-$ to one of the stable manifolds of $\mathbf{x}^*_+$. A finite ϵ removes the mirror line $y = 0$, present at $\epsilon = 0$, and destroys the heteroclinic orbit. Real world systems are often devoid of symmetries and heteroclinic orbits hence rare.

2.2.2 Bifurcations and Normal Forms

The nature of the solutions to a dynamical system, as defined by a suitable first order differential equation (2.6), may change qualitatively as a function of some control parameter a. When this happens one speaks of a "bifurcation". Here we the most important classes. For this purpose we consider a selection

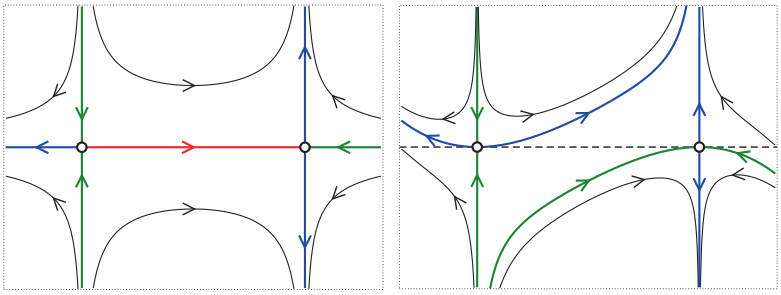

Fig. 2.6 Sample trajectories of the system (2.18). for $\epsilon = 0$ (left) and $\epsilon = 0.2$ (right). Shown are the stable manifolds (thick green lines), the unstable manifolds (thick blue lines) and the heteroclinic orbit (thick red line).

of simple equations, which can be viewed as archetypical, and to which more complex dynamical systems will generically reduce close to the transition point.

Saddle-node Bifurcation We consider the dynamical system defined by

$$\frac{dx}{dt} = a - x^2 \ , \tag{2.19}$$

for a real variable x and a real control parameter a. The fixpoints $\dot{x} = 0$

$$x_+^* = +\sqrt{a}, \qquad x_-^* = -\sqrt{a}, \qquad a > 0 \tag{2.20}$$

exist only for positive control parameters, $a > 0$; there are no fixpoints for negative $a < 0$. For the flow we find

$$\frac{dx}{dt} = \begin{cases} < 0 & \text{for} \quad x > \sqrt{a} \\ > 0 & \text{for} \quad x \in [-\sqrt{a}, \sqrt{a}] \\ < 0 & \text{for} \quad x < -\sqrt{a} \end{cases} \tag{2.21}$$

for $a > 0$. The upper branch x_+^* is hence stable and the lower branch x_-^* unstable, as illustrated in Fig. 2.7.

For a saddle-node bifurcation a stable and an unstable fixpoint collide and annihilate each other, one speaks also of a fold, tangential or blue sky bifurcation.

Transcritical Bifurcation We now consider the dynamical system

$$\frac{dx}{dt} = ax - x^2 \ , \tag{2.22}$$

again for a real variable x and a real control parameter a. The two fixpoint solutions $\dot{x} = 0$,

$$x_0^* = 0, \qquad x_a^* = a, \qquad \forall a \tag{2.23}$$

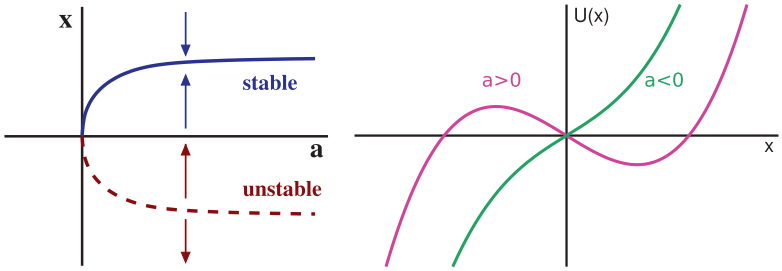

Fig. 2.7 The saddle-node bifurcation, as described by Eq. (2.19). There are two fixpoints for $a > 0$, an unstable branch $x^*_- = -\sqrt{a}$ and a stable branch $x^*_+ = +\sqrt{a}$. **Left:** The phase diagram together with the flow (arrows). **Right:** The bifurcation potential $U(x) = -ax + x^3/3$, compare Eq. (2.25).

exist for all values of the control parameter. The direction of the flow $\dot{x}$ is positive for x in between the two solutions and negative otherwise, see Fig. 2.8. The respective stabilities of the two fixpoint solutions exchange consequently at $a = 0$.

Bifurcation Potentials In many cases one can write the dynamical system under consideration, in analogy to the Newton equation of motion of classical dynamics, as

$$\frac{dx}{dt} = -\frac{d}{dx}\,U(x)\ , \tag{2.24}$$

where $U(x)$ is the potential. Local minima of the potential then correspond to stable fixpoints, compare Fig. 2.2. The potentials for the saddle-node and the transcritical bifurcation are

$$U_{saddle}(x) = -ax + \frac{1}{3}x^3, \qquad U_{trans}(x) = -\frac{a}{2}x^2 + \frac{1}{3}x^3\ , \tag{2.25}$$

respectively, see the definitions (2.19) and (2.22). The bifurcation potentials, as shown in Figs. 2.7 and 2.8, bring immediately to evidence the stability of the respective fixpoints.

Pitchfork Bifurcation The "supercritical" pitchfork bifurcation is described by

$$\frac{dx}{dt} = ax - x^3, \qquad x^*_0 = 0, \qquad x^*_+ = +\sqrt{a}, \qquad x^*_- = -\sqrt{a}\ . \tag{2.26}$$

A trivial fixpoint $x^*_0 = 0$ becomes unstable at criticality, $a = 0$, and two symmetric stable fixpoints appear, see Fig. 2.9. The respective bifurcation potential,

$$U_{pitch}(x) = -\frac{a}{2}x^2 + \frac{1}{4}x^4\ , \tag{2.27}$$

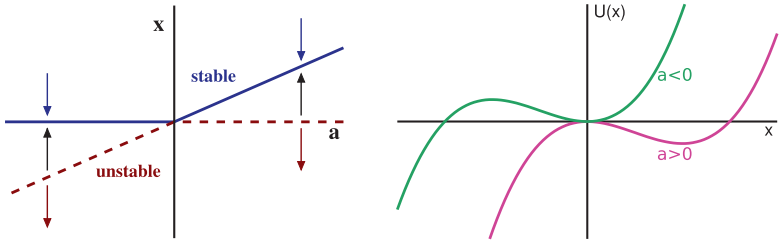

Fig. 2.8 The transcritical bifurcation, see Eq. (2.22). The two fixpoints $x_0^* = 0$ and $x_a^* = a$ exchange stability at $a = 0$. **Left:** Phase diagram and flow (arrows). **Right:** The bifurcation potential $U(x) = -ax^2/2 + x^3/3$, compare Eq. (2.25).

is identical to the Landau-Ginzburg potential describing second-order phase transitions in statistical physics, which we will discuss, in the context of self-organized criticality, in Sect. 6.1. of Chap. 6, "Cellular Automata and Self-Organized Criticality". One also considers the subcritical pitchfork transition defined by $\dot{x} = ax + x^3$. We leave the discussion to the reader.

Bifurcation Symmetries The three bifurcation scenarios discussed above, saddle-node, transcritical and pitchfork, are characterized by their symmetries close to the critical point, which has been set to $x = 0$ and $a = 0$ for all three cases. The normal forms, such as (2.26), and their respective bifurcation potentials, constitute the simplest formulations consistent with the defining symmetry properties.

The bifurcation potentials of the saddle-node and the pitchfork transitions are respectively antisymmetric and symmetric under a sign change $x \leftrightarrow -x$ of the dynamical variable, compare Eqs. (2.25) and (2.27).

$(+) \leftrightarrow (-)$	saddle-node	transcritical	pitchfork
x	anti	–	symm
a, x	–	anti	–

The bifurcation potential of the transcritical bifurcation is, on the other hand, antisymmetric under the combined symmetry operation $x \leftrightarrow -x$ and $a \leftrightarrow -a$, compare Eq. (2.25).

2.2.3 Hopf Bifurcations and Limit Cycles

Hopf Bifurcation A Hopf bifurcation occurs when a fixpoint changes its stability together with the appearance of an either stable or unstable limiting cycle, e.g. as for non-linear rotator illustrated in Fig. 2.1. The canonical equations of motions are

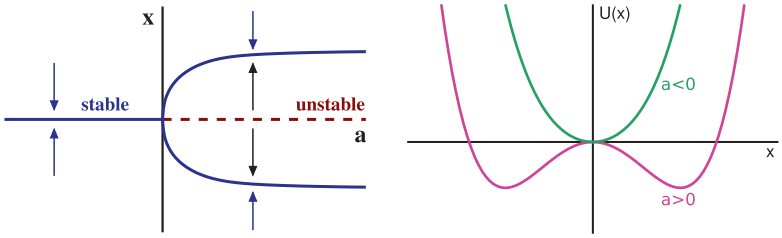

Fig. 2.9 The supercritical pitchfork bifurcation, as defined by Eq. (2.26). The t$x_0^* = 0$ becomes unstable for $a > 0$ and two new stable fixpoints, $x_+^* = +\sqrt{a}$ and $x_-^* = -\sqrt{a}$ appear. **Left:** Phase diagram and flow (arrows). **Right:** The bifurcation potential $U(x) = -ax^2/2 + x^4/4$, compare Eq. (2.25).

$$\begin{aligned} \dot{x} &= -y + d(\Gamma - x^2 - y^2)\, x \\ \dot{y} &= \quad x + d(\Gamma - x^2 - y^2)\, y \end{aligned} \tag{2.28}$$

in Euclidean phase space $(x, y) = (r\cos\varphi, r\sin\varphi)$, which reduce to the nonlinear rotator of Eq. (2.2) when setting $d \to 1$. There are two steady-state solutions for $\Gamma > 0$,

$$(x_0^*, y_0^*) = (0, 0), \qquad (x_\Gamma^*, y_\Gamma^*) = \sqrt{\Gamma}\,(\cos(t), \sin(t)) \ , \tag{2.29}$$

a fixpoint and a limit cycle. The limit cycle disappears for $\Gamma < 0$.

Supercritical Hopf Bifurcations For $d > 0$ the bifurcation is denoted "supercritical". The fixpoint $\mathbf{x}_0^* = (x_0^*, y_0^*)$ is stable/unstable for $\Gamma < 0$ and $\Gamma > 0$ and the limit cycle $\mathbf{x}_\Gamma^* = (x_\Gamma^*, y_\Gamma^*)$ is stable, as illustrated in Fig. 2.1.

Subcritical Hopf Bifurcations The direction of flow is reversed for $d < 0$, with respect to the supercritical Hopf bifurcation illustrated in Fig. 2.1, and the limit cycle $\mathbf{x}_\Gamma^*$ becomes repelling. The fixpoint $\mathbf{x}_0^*$ is then unstable/stable for $\Gamma < 0$ and $\Gamma > 0$, one speaks of a "subcritical" Hopf bifurcation as a function of the bifurcation parameter Γ.

Hopf Bifurcation Theorem One may be interested to find out whether a generic two dimensional system

$$\begin{aligned} \dot{x} &= f_\mu(x, y) \\ \dot{y} &= g_\mu(x, y) \end{aligned} \ . \tag{2.30}$$

can be reduced to the normal form (2.28) for a Hopf bifurcation, where μ is the bifurcation parameter. Without loss of generality one can assume that the fixpoint $\mathbf{x}_0^*$ stays at the origin for all values of μ and that the transition takes place for $\mu = 0$.

To linear order the normal form (2.28) and (2.30) are equivalent if the Jacobian of (2.30) has a pair of complex conjugate eigenvalues, with the real

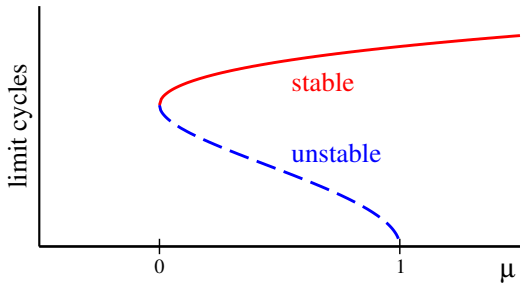

Fig. 2.10 The locations $R_\pm = \sqrt{1 \pm \sqrt{\mu}}$ of the stable and unstable limit cycles, R_- and R_+, for the non-linear rotator (2.31) and the parametrization (2.32). At $\mu = 0$ a fold bifurcation of limit cycles occurs and a subcritical Hopf bifurcation at $\mu = 1$, compare Fig. 2.11.

value crossing with a finite slope zero at $\mu = 0$, corresponding to a transition from a stable to an unstable focus.

Comparing (2.28) and (2.30) to quadratic order one notices that quadratic terms are absent in the normal form (2.28) but not in (2.30). One can however show, with the help of a suitable non-linear transformation, that it is possible to eliminate all quadratic terms from (2.30).

The nature of the bifurcation is determined by a combination of partial derivatives up to cubic order,

$$\begin{aligned} a = &\left[f_{xxx} + f_{xyy} + g_{xxy} + g_{yyy}\right]/16 \\ &+ \left[f_{xy}(f_{xx} + f_{yy}) - g_{xy}(g_{xx} + g_{yy}) - f_{xx}g_{xx} - f_{yy}g_{yy}\right]/(16\omega) \end{aligned}$$

where $\omega > 0$ is the imaginary part of the Lyapunov exponent at the critical point $\mu = 0$ and where the partial derivatives as f_{xy} are to be evaluated at $\mu = 0$ and $\mathbf{x} \to \mathbf{x}_0^*$. The Hopf bifurcations is supercritical and subcritical respectively for $a < 0$ and $a > 0$.

Interplay Between Multiple Limit Cycles A dynamical system may dispose generically of a number of limit cycles, which may merge or disappear as a function of a given parameter. Here we consider the simplest case, generalizing the non-linear rotator (2.2) to next order in r^2,

$$\dot{r} = -(r^2 - \gamma_-)(r^2 - \gamma_+)\, r, \qquad \dot{\varphi} = \omega, \qquad \gamma_- \le \gamma_+ \,. \tag{2.31}$$

Real-world physical or biological systems have bounded trajectories and $\dot{r}$ must be negative for large radii $r \to \infty$. This requirement has been taken into account in (2.31), which is also called the "Bautin normal form".

For $\gamma_- < 0$ the first factor $(r^2 - \gamma_-)$ is smooth for $r^2 \ge 0$ and does not influence the dynamics qualitatively. In this case (2.31) reduces to the supercritical Hopf bifurcation, as a function of the bifurcation parameter γ_+ (Fig. 2.10).

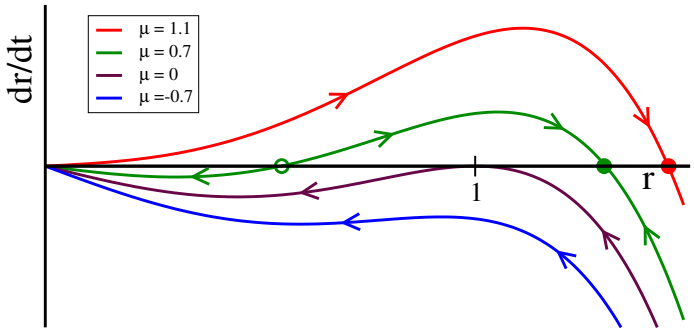

Fig. 2.11 Flow diagram for the non-linear rotator (2.31) using the parametrization (2.32) for the roots of r^2. The filled/open circles denote stable/unstable limit cycles. For $\mu \to 1$ the unstable limit cycle vanishes, a subcritical Hopf bifurcation. The stable and the unstable limit cycle collided for positive $\mu \to 0$ and annihilate each other, a fold bifurcation of limit cycles.

Phenomenological Parametrization The roots $\gamma_\pm$ of r^2 in (2.31) typically result from some determining relation. As a possible simple assumption we consider a quadratic relation of the form

$$\gamma_\pm = 1 \pm \sqrt{\mu} \;, \tag{2.32}$$

where μ will be our bifurcation parameter. For $\mu \in [0, 1]$ we have two positive roots and consequently also two limit cycles, a stable and an unstable one. For $\mu \to 1$ the unstable limit cycle vanishes in a subcritical Hopf bifurcation, compare Fig. 2.11.

Fold Bifurcation of Limit Cycles For a saddle-node bifurcation of fixpoints, also termed "fold bifurcation", a stable and an unstable fixpoint merge and annihilate each other, as illustrated in Fig. 2.7. The equivalent phenomenon may occur for limit cycles, as shown in Fig. 2.11 and happens in our model when μ becomes negative,

$$\gamma_\pm = 1 \pm i\sqrt{|\mu|}, \qquad \dot{r} = -\big[(r^2-1)^2 + |\mu|\big] r \;.$$

No limit cycle exists anymore for $\mu \leq 0$, only a stable fixpoint at $r_0^* = 0$ remains.

2.3 Global Bifurcations

The bifurcations discussed in Sect. 2.2.3 can be termed "local" as they are based on Taylor expansions around a local fixpoint, and the dynamical state changes smoothly at the bifurcation point. There are, on the other hand,

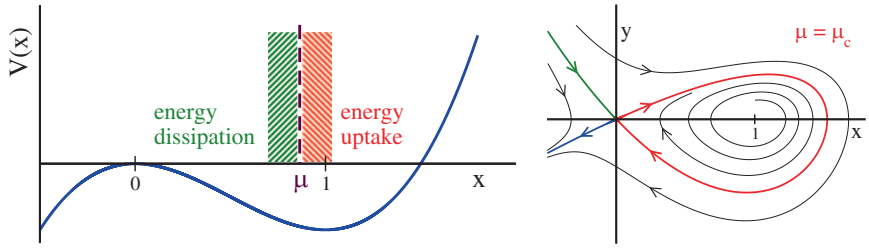

Fig. 2.12 Left: The potential $V(x)$ of the Taken-Bogdanov system (2.33). Energy is dissipated to the environment for $x < \mu$ and taken up for $x > \mu$. The value for μ illustrated in the figure is the critical $\mu_c \approx 0.8645$. For $\mu < 1$ the local minimum $x = 1$ of the potential becomes an unstable focus. **Right:** The flow for $\mu = \mu_c$. The stable and unstable manifolds form an homoclinic loop (red line).

bifurcations characterized by the properties of extended orbits. These kinds of bifurcations are hence of "global" character.

Taken-Bogdanov System We consider a mechanical system with a cubic potential $V(x)$ and velocity-dependent forces,

$$\begin{aligned} \ddot{x} &= (x-\mu)\dot{x} - V'(x) & \dot{x} &= y \\ V(x) &= x^3/3 - x^2/2 & \dot{y} &= (x-\mu)y + x(1-x) \end{aligned} \quad . \tag{2.33}$$

The conservative contribution to the force field is $-V'(x) = x(1-x)$. An illustration of the potential $V(x)$ is presented in Fig. 2.12.

For $x < \mu$ the term $(x-\mu)\dot{x}$ in (2.33) reduces the velocity, and the energy

$$E = \frac{\dot{x}^2}{2} + V(x), \qquad \frac{dE}{dt} = \left[\ddot{x} + V'(x)\right]\dot{x} = (x-\mu)\dot{x}^2 \tag{2.34}$$

is dissipated. If, however, $x > \mu$, then energy is taken up and the term $(x-\mu)\dot{x}$ results in an acceleration. This interplay between energy dissipation and uptake is typical for adaptive systems, which will be discussed further in Sect. 3.1.3 of Chap. 3, "Dissipation, Noise and Adaptive Systems".

Fixpoints and Jacobian The Taken-Bogdanov system (2.33) has two fixpoints $(x^*, 0)$, with $x^* = 0, 1$, and the Jacobian

$$J = \begin{pmatrix} 0 & 1 \\ (1-2x^*) & (x^*-\mu) \end{pmatrix}, \qquad \begin{aligned} \lambda_\pm(0,0) &= -\mu/2 \pm \sqrt{\mu^2/4 + 1} \\ \lambda_\pm(1,0) &= (1-\mu)/2 \pm \sqrt{(1-\mu)^2/4 - 1} \end{aligned}$$

The fixpoint $(0,0)$ is always a saddle, since the mechanical potential $V(x)$ has a quadratic maximum at $x = 0$.

The local minimum $(1,0)$ of the potential is a stable/unstable focus for $\mu > 1$ and $\mu < 1$ respectively, with $\mu = 1$ being the locus of a supercritical Hopf

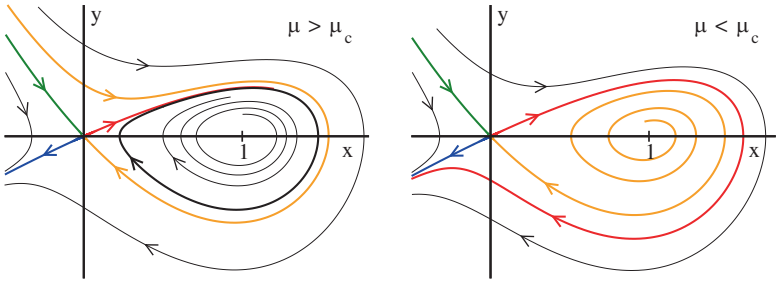

Fig. 2.13 The flow for the Taken-Bogdanov system (2.33), the critical bifurcation parameter is $\mu_c \approx 0.8645$. **Left:** The flow in the subcritical region, for $\mu = 0.9 > \mu_c$, together with the resulting limit cycle (thick black line) For $\mu \to \mu_c$ the and unstable (red) and stable (orange) and manifolds join to form a homoclinic loop which is, at the same time, identical with the locus of the limit cycle for $\mu \to \mu_c$. **Right:** The flow in the supercritical region, for $\mu = 0.8 < \mu_c$. The limit cycle has broken after touching the saddle at $(0, 0)$.

bifurcation. We consider now $\mu \in [0, 1]$ and examine the further evolution of the resulting limit cycle.

Escaping the Potential Well We consider a particle starting with a vanishing velocity close to $x = 1$, the local minimum of the Potential well.

When the particle takes up enough energy from the environment, due to the velocity dependent force $(x - \mu)v$, it will be able to reach the local maximum at $x = 0$ and escape to $x \to -\infty$. This is the case for $\mu < \mu_c \approx 0.8645$ and all orbits will escape.

The particle remains trapped in the local potential well if, on the other side, dissipation dominates, which is the case for $\mu > \mu_c$. The particle is both trapped in the local well and repelled, at the same time, from the unstable minimum at $x = 1$, if $\mu < 1$ holds additionally. The orbit hence performs an oscillatory motion for $\mu \in [\mu_c, 1]$, with the trajectory in phase space (x, y) approaching a limit cycle. This limit cycle increases in size for decreasing $\mu \to \mu_c$, exactly touching $(0, 0)$ for $\mu = \mu_c$, and breaking apart for $\mu < \mu_c$, as illustrated in Fig. 2.13.

The bifurcation occurring at $\mu = \mu_c$ depends non-locally on the overall energy balance and is therefore an example of a global bifurcation.

Homoclinic Bifurcation With a "homocline" one denotes a loop formed by joining a stable and an unstable manifold of the same fixpoint. Homoclines may generically only occur if either forced by symmetries or for special values of bifurcation parameters, with the later being the case for Taken-Bogdanov system.

An unstable and a stable manifold cross at $\mu = \mu_c$, compare Figs. 2.12 and 2.13, forming a homocline. The homocline is also the endpoint of the limit cycle present for $\mu > \mu_c$, which disappears for $\mu < \mu_c$. One speaks of a homoclinic bifurcation, an incidence of a global bifurcation. The limit

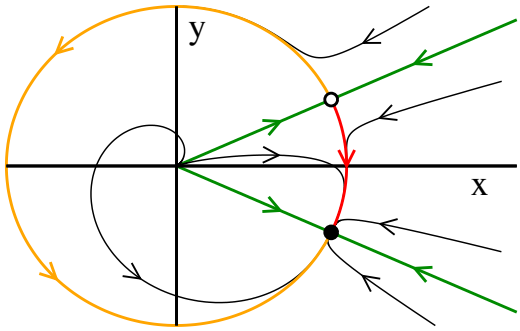

Fig. 2.14 The flow for a system showing an infinite period bifurcation, as defined by Eqs. (2.35) and (2.36), and for $K = 1.1$. The stable fixpoint (filled circle) merges with the saddle (open cicle) in the limit $K \to 1$, thus showing a saddle-node bifurcation on an invariant cycle.

cycle is destroyed when maximal for a homoclinic bifurcation, and not when minimal, as for a supercritical Hopf bifurcation.

Coupled Oscillators For a further example of how a limit cycle may disappear discontinuously we consider two coupled harmonic oscillators within the Kuramoto model[1], having individual phases, respectively θ_1 and θ_2. A typical evolution equation for the phase difference $\varphi = \theta_1 - \theta_2$ is then

$$\dot{\varphi} = 1 - K\cos(\varphi) \ . \tag{2.35}$$

We can interpret (2.35) via

$$\dot{r} = \left(1 - r^2\right) r, \qquad x = r\cos(\varphi), \qquad y = r\sin(\varphi) \tag{2.36}$$

within the context of a two dimensional limit cycle, compare Eq. (2.2).

The phase difference φ continuously increases for $|K| < 1$ and the system settles into a limit cycle. For $|K| > 1$ two fixpoints for $\dot{\varphi} = 0$ appear, a saddle and a stable node, as illustrated in Fig. 2.14, and the limit cycle is broken up.

Infinite Period Bifurcation The limit cycle for $|K| < 1$ has a revolution period T of

$$T = \int_0^T dt = \int_0^{2\pi} \frac{dt}{d\varphi} d\varphi = \int_0^{2\pi} \frac{d\varphi}{\dot{\varphi}} = \int_0^{2\pi} \frac{d\varphi}{1 - K\cos(\varphi)} = \frac{2\pi}{\sqrt{1 - K^2}} \ ,$$

which diverges in the limit $|K| \to 1$. The global transition occurring at $|K| = 1$ is termed "infinite period bifurcation", being characterized by a diverging time scale.

[1] The Kuramoto model is discussed in detail in Sect. 9.1 of Chap. 9, "Synchronization Phenomena".

2.3.1 Catastrophe Theory

A catchy terminology for potentially discontinuous bifurcations in dynamical systems is "catastrophe theory", especially when placing emphasis on a geometric interpretation. Catastrophe theory is interested in bifurcations with "codimension" two or higher.

CODIMENSION. The degrees of freedom characterizing a bifurcation diagram.

The codimension corresponds, colloquially speaking, to the number of parameters one may vary such that something interesting happens. All bifurcation normal forms discussed in Sect. 2.2.2 had a codimension of one.

Pitchfork Bifurcation with a Symmetry Breaking Term We consider a one-dimensional system,

$$\dot{x} = h + ax - x^3 \ . \tag{2.37}$$

For $h = 0$ the system reduces to the pitchfork normal form of Eq. (2.26), and (2.37) is then invariant under the parity transformation $x \leftrightarrow -x$.

Parity is broken whenever $h \neq 0$ and (2.37) can hence be considered as the simplest case allowing to study the influence of symmetry breaking onto a bifurcation diagram. There are two free parameters, h and a, the codimension is hence two.

Pitchfork Bifurcation and Phase Transitions The pitchfork system (2.37) has a close relation to the theory of thermodynamic phase transitions[2], when assuming that

$$a = a(T) = a_0(T_c - T), \qquad a_0 > 0 \ ,$$

where T is the temperature of the system.

There is, in the absence of an external field h, only a single fixpoint x^* for $T > T_c$, viz for temperatures above the critical temperature T_c. In the ordered state, for $T < T_c$, there are two possible phases, characterized by the positive and negative stable fixpoint x^* respectively.

Hysteresis and Memory The behavior of the phase transition changes when an external field h is present. Switching the sign of the field is accompanied, in the ordered state for $T < T_c$, with a "hysteresis-loop"

$$(1) \rightarrow (2) \rightarrow (3) \rightarrow (4) \rightarrow \ldots \ ,$$

as illustrated in Fig. 2.15.

– The field h changes from negative to positive values along (1) → (2), with the fixpoint x^* remaining negative.

[2] The Landau theory of phase transitions is discussed in Sect. 6.1 of Chap. 6, "Cellular Automata and Self-Organized Criticality".

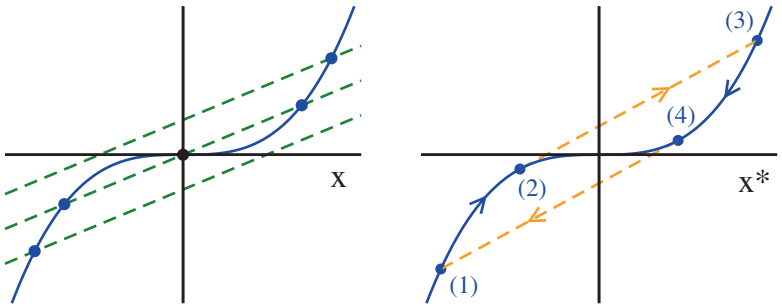

Fig. 2.15 Left: The self-consistency condition $x^3 = h + ax$ for the fixpoints x^* of the symmetry broken pitchfork system (2.37), for various fields h and a positive $a > 0$. The unstable fixpoint at $x = 0$ becomes stable for $a < 0$, compare Fig. 2.9. **Right:** The hysteresis loop (1) → (2) → (3) → (4) → ... occurring for $a > 0$ as function of the field h.

– At (2) the negative stable fixpoint disappears and the system makes a rapid transition to (3), the catastrophe.
– Lowering eventually again the field h, the system moves to (4), jumping in the end to (1).

The system retains its state, x^* being positive or negative, to a certain extend and one speaks of a memory in the context of catastrophe theory.

Center Manifold A d-dimensional dynamical system with a fixpoint $\mathbf{x}^*$ and a Jacobian J,

$$\dot{\mathbf{x}} = \mathbf{f}(\mathbf{x}), \qquad J_{ij} = \frac{\partial f_i}{\partial x_j}\Big|_{\mathbf{x}=\mathbf{x}^*}, \qquad J\mathbf{e}_n = \lambda_n \mathbf{e}_n \ ,$$

may have a number of neutral Lyapunov exponents with vanishing eigenvalues $\lambda_i = 0$ of the Jacobian.

CENTER MANIFOLD. The space spanned by the neutral eigenvectors $\mathbf{e_i}$ is denoted the center manifold.

Catastrophe theory deals with fixpoints having a non-vanishing center manifold.

Center Manifold for the Pitchfork System The Lyapunov exponent

$$\lambda = a - 3\,(x^*)^2$$

of the pitchfork system (2.37) vanishes at the jump-points (2) and (4) at which the catastrophe occurs, compare Fig. 2.15. At the jump-points $h + ax$ is per definition tangent to x^3, having identical slopes:

$$\frac{d}{dx}x^3 = \frac{d}{dx}\big(h + ax\big), \qquad 3x^2 = a \ . \tag{2.38}$$

At these transition points the autonomous flow becomes hence infinitesimally slow, since $\lambda \to 0$, a phenomenon called "critical slowing down" in the context of the theory of thermodynamic phase transitions.

Center Manifold Normal Forms The program of the catastrophe theory consists of finding and classifying the normal forms for the center manifolds of stationary points $\mathbf{x}^*$, by expanding to the next, non-vanishing order in $\delta\mathbf{x} = \mathbf{x} - \mathbf{x}^*$. The aim is hence to classify the types of dynamical behavior potentially leading to discontinuous transitions.

Catastrophic Fixpoints A generic fixpoint $\mathbf{x}^* = \mathbf{x}^*(\mathbf{c})$ depends on control parameters $\mathbf{c} = (c_i, .., c_S)$ of the equations of motion, with S being the codimension. The flow is however smooth around a generic fixpoint and a finite center manifold arises only for certain sets $\{c_i^c\}$ of control parameters.

The controlling parameters of the pitchfork system (2.37) are h and a, in our example system, and a center manifold exists only when (2.38) is fulfilled, viz when

$$3\left[x^*(h^c, a^c)\right]^2 = a^c, \qquad x^*(h^c, a^c) = x_c^*$$

holds, which determines the set of "catastrophic fixpoints" x_c^*.

Changing the Controlling Parameters How does the location $\mathbf{x}^*$ of a fixpoint change upon variations $\delta\mathbf{c}$ around the set of parameters $\mathbf{c}^c$ determining the catastrophic fixpoint $\mathbf{x}_c^*$? With

$$\mathbf{x}_c^* = \mathbf{x}^*(\mathbf{c}^c), \qquad \mathbf{x}^* = \mathbf{x}^*(\mathbf{c}), \qquad \delta\mathbf{c} = \mathbf{c} - \mathbf{c}^c$$

we expand the fixpoint condition $\mathbf{f}(\mathbf{x}, \mathbf{c}) = 0$ and obtain

$$J\delta\mathbf{x}^* + P\delta\mathbf{c} = 0, \qquad J_{ij} = \frac{\partial f_i}{\partial x_j}, \qquad P_{ij} = \frac{\partial f_i}{\partial c_j}\ , \tag{2.39}$$

which we can invert if the Jacobian J is non-singular,

$$\delta\mathbf{x}^* = -J^{-1}P\delta\mathbf{c}, \qquad \text{if} \qquad |J| \neq 0\ . \tag{2.40}$$

The fixpoint may change however in a discontinuous fashion whenever the determinant $|J|$ of the Jacobian vanishes, viz in the presence of a center manifold. This is precisely what happens at a catastrophic fixpoint $\mathbf{x}_c^*(\mathbf{c}^c)$.

Catastrophic Manifold The set $\mathbf{x}_c^* = \mathbf{x}_c^*(\mathbf{c}^\mathbf{c})$ of catastrophic fixpoints is determined by two conditions, by the fixpoint condition $\mathbf{f} = 0$ and by $|J| = 0$. For the pitchfork system (2.37) we find,

$$a_c = 3\,(x_c^*)^2\,, \qquad h_c = (x_c^*)^3 - a_c x_c^* = -2\,(x_c^*)^3\ ,$$

when using (2.38). Solving for $x_c^* = \sqrt{a_c/3}$ we can eliminate x_c^* and obtain

$$h_c = -2\,(a_c/3)^{3/2}\,, \qquad (h_c/2)^2 = (a_c/3)^3\ , \tag{2.41}$$

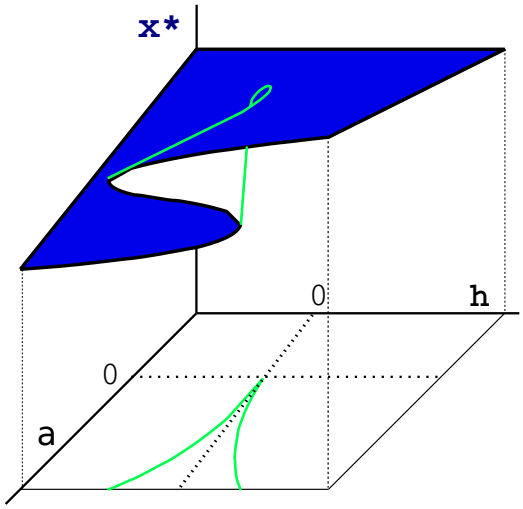

Fig. 2.16 The fixpoints x^* (upper folded plane) of the symmetry broken pitchfork system (2.37), as a function of the control parameters a and h. The catastrophic manifold (a_c, h_c), compare Eq. (2.41), has a cusp-like form (green lines).

which determines the "catastrophic manifold" (a_c, h_c) for the pitchfork transition, as illustrated in Fig. 2.16.

Classification of Perturbations The control parameters (a_c, h_c) of the pitchfork transition may be changed in two qualitatively distinct ways, namely along the catastrophic manifold (2.41), or perpendicular to it.

It would hence be useful to dispose of a list of canonical perturbations characterizing all possible distinct routes to change catastrophic fixpoints $x_c^* = x^*(\mathbf{c}^c)$ qualitatively, upon small changes $\delta\mathbf{c} = \mathbf{c} - \mathbf{c}^c$ of the control parameters $\mathbf{c}$. It is the aim of catastrophe theory to develop such a canonical classification scheme for the perturbations of center manifolds.

Gradient Dynamical Systems At times the flow $\mathbf{f}(\mathbf{x})$ of a dynamical system may be represented as a gradient of a bifurcation potential $U(\mathbf{x})$,

$$\dot{\mathbf{x}} = \mathbf{f}(\mathbf{x}) = -\nabla U(\mathbf{x}) \ . \tag{2.42}$$

This is generically the case for one-dimensional systems, as discussed in Sect. 2.2.2, but otherwise not. For the gradient representation

$$\begin{aligned} \dot{x} &= g(x,y) \qquad & g &= -U_x(x,y) \\ \dot{y} &= h(x,y) \qquad & h &= -U_y(x,y) \end{aligned}$$

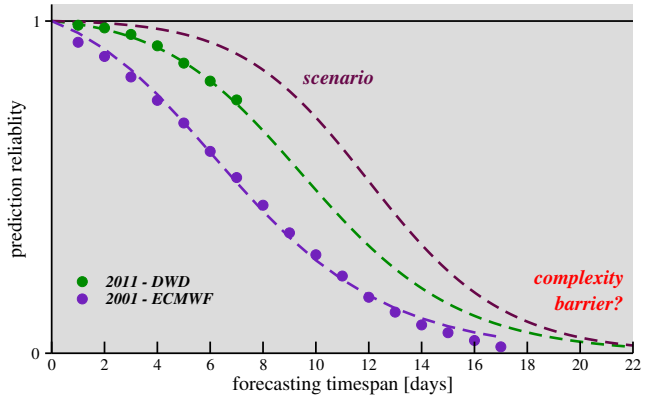

Fig. 2.17 The average accuracy of weather forecasting, normalized to $[0, 1]$, decreases rapidly with increasing prediction timespan, due to the chaotic nature of weather dynamics. Increasing the resources devoted for improving the prediction accuracy results in decreasing returns close to the resulting complexity barrier (From Gros (2012)).

of a two-dimensional system to be valid, to give an example, the cross-derivatives $g_y = -U_{xy} = -U_{yx} = h_x$ would need to coincide. This is however normally not the case.

For gradient dynamical systems one needs to discuss only the properties of the bifurcation potential $U(\mathbf{x})$, as scalar quantity, and they are hence somewhat easier to investigate than a generic dynamical system of the form $\dot{\mathbf{x}} = \mathbf{f}(\mathbf{x})$. Catastrophe theory is mostly limited to gradient systems.

2.4 Logistic Map and Deterministic Chaos

Chaos The notion of "chaos" plays an important role in dynamical systems theory. A chaotic system is defined as a system that cannot be predicted within a given numerical accuracy. At first sight this seems to be a surprising concept, since differential equations of the type of Eq. (2.6), which do not contain any noise or randomness, are perfectly deterministic. Once the starting point is known, the resulting trajectory can be calculated for all times. Chaotic behavior can arise nevertheless, due to an exponential sensitivity to initial conditions.

> Deterministic Chaos. A deterministic dynamical system showing exponential sensibility of the time development on the initial conditions is called chaotic.

This means that a very small change in the initial setting can blow up even after a short time. When considering real-world applications, when models need to be determined from measurements containing inherent errors and limited accuracies, an exponential sensitivity can result in unpredictability.

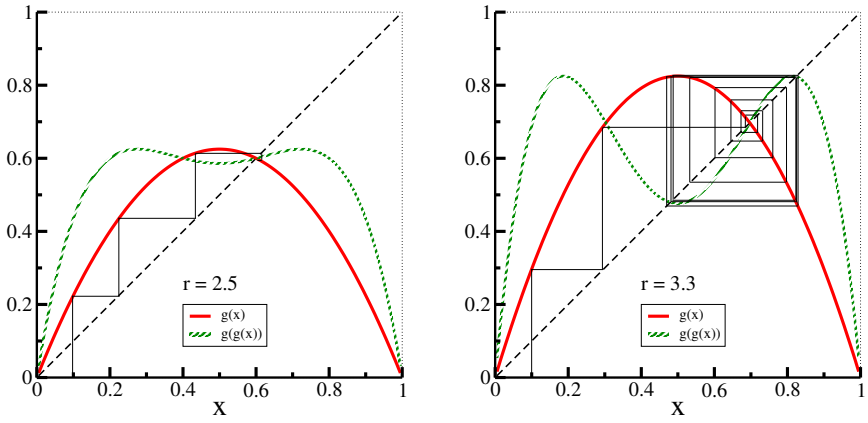

Fig. 2.18 Illustration of the logistic map $g(x) = rx(1-x)$ (red), and of the iterated logistic map $g(g(x))$ (green); for $r=2.5$ (left) and $r=3.3$ (right). Also shown is an iteration of $g(x)$, starting from $x=0.1$ (thin solid line) Note, that the fixpoint $g(x) = x$ is stable/unstable for $r=2.5$ and $r=3.3$, respectively. The orbit is attracted to a fixpoint of $g(g(x))$ for $r=3.3$, corresponding to a cycle of period two for $g(x)$.

A well known example is the problem of long-term weather prediction, as illustrated in Fig. 2.17.

Logistic Map One of the most cherished models in the field of deterministic chaos is the logistic map of the interval $[0, 1]$ onto itself:

$$x_{n+1} = g(x_n) \equiv r\, x_n\, (1 - x_n), \qquad x_n \in [0, 1], \qquad r \in [0, 4]\ , \tag{2.43}$$

where we have used the notation $x_n = x(n)$, for discrete times $n = 0,\ 1,\ ..\ .$ The functional dependence is illustrated in Fig. 2.18. Despite its apparent simplicity, the logistic map shows an infinite series of bifurcations that culminate in a transition to chaos.

Biological Interpretation We may consider $x_n \in [0, 1]$ as standing for the population density of a reproducing species in the year n. In this case the factor $r(1 - x_n) \in [0, 4]$ corresponds to the number of offspring per year and animal, which is limited in the case of high population densities $x \to 1$, viz when resources become scarce. The classical example is that of a herd of reindeer on an island.

Knowing the population density x_n in a given year n we may predict via Eq. (2.43) the population density for all subsequent years exactly; the system is deterministic. Nevertheless the population shows irregular behavior for certain values of r, which one calls "chaotic".

Fixpoints of the Logistic Map We start considering the fixpoints of $g(x)$:

$$x = rx(1 - x) \qquad \Longleftrightarrow \qquad x = 0 \quad \text{or} \quad 1 = r(1 - x)\ .$$

The non-trivial fixpoint is then

$$1/r = 1 - x, \qquad x^{(1)} = 1 - 1/r, \qquad r_1 < r, \qquad r_1 = 1\ . \tag{2.44}$$

It occurs only for $r_1 < r$, with $r_1 = 1$, due to the restriction $x^{(1)} \in [0, 1]$.

Stability of the Fixpoint For maps, fixpoints are stable when the derivative g' of the flow is smaller than one in magnitude, see (2.14) For $x^{(1)} = 1 - 1/r$ this translates to

$$g'(x) = r(1 - 2x), \qquad g'\left(x^{(1)}\right) = 2 - r\,. \tag{2.45}$$

Noting that $r \in [1, 4]$, we obtain

$$|2 - r| < 1 \quad \Longleftrightarrow \quad \boxed{r_1 < r < r_2} \qquad \begin{matrix} r_1 = 1 \\ r_2 = 3 \end{matrix} \tag{2.46}$$

for the region of stability of $x^{(1)}$.

Fixpoints of Period Two For $r > 3$ a fixpoint of period two appears. This fixpoint is is a fixpoint of the iterated function

$$g(g(x)) = rg(x)(1 - g(x)) = r^2x(1 - x)(1 - rx(1 - x))\,.$$

The fixpoint equation $x = g(g(x))$ leads to the cubic equation

$$\begin{aligned} 1 &= r^2(1 - rx + rx^2) - r^2x(1 - rx + rx^2), \\ 0 &= r^3x^3 - 2r^3x^2 + (r^3 + r^2)x + 1 - r^2\ . \end{aligned} \tag{2.47}$$

In order to find the roots of Eq. (2.47) we use the fact that $x = x^{(1)} = 1 - 1/r$ is a stationary point of both $g(x)$ and $g(g(x))$, see Fig. 2.18. We divide (2.47) by the root $(x - x^{(1)}) = (x - 1 + 1/r)$:

$$\begin{gathered} (r^3x^3 - 2r^3x^2 + (r^3 + r^2)x + 1 - r^2) : (x - 1 + 1/r) \ = \\ r^3x^2 - (r^3 + r^2)x + (r^2 + r)\ . \end{gathered}$$

The two new fixpoints of $g(g(x))$ are therefore the roots of

$$x^2 - \left(1 + \frac{1}{r}\right)x + \left(\frac{1}{r} + \frac{1}{r^2}\right) = 0\ .$$

We obtain

$$x_{\pm}^{(2)} = \frac{1}{2}\left(1 + \frac{1}{r}\right) \pm \sqrt{\frac{1}{4}\left(1 + \frac{1}{r}\right)^2 - \left(\frac{1}{r} + \frac{1}{r^2}\right)}\ . \tag{2.48}$$

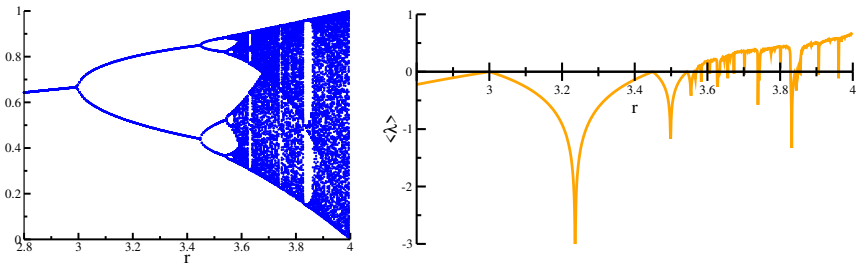

Fig. 2.19 Left: The values x_n for the iterated logistic map (2.43). For $r < r_\infty \approx 3.57$ the x_n go through cycles with finite but progressively longer periods. For $r > r_\infty$ the plot would be fully covered in most regions, if all x_n would be shown. **Right:** The corresponding maximal Lyapunov exponents, as defined by Eq. (2.52). Positive Lyapunov exponents λ indicate chaotic behavior.

Bifurcation We have three fixpoints for $r > 3$ (two stable ones and one unstable), and only one fixpoint for $r < 3$. What happens for $r = 3$?

$$x_\pm^{(2)}(r=3) = \frac{1}{2}\frac{3+1}{3} \pm \sqrt{\frac{1}{4}\left(\frac{3+1}{3}\right)^2 - \left(\frac{3+1}{9}\right)}$$
$$= \frac{2}{3} = 1 - \frac{1}{3} = x^{(1)}(r=3)\ .$$

At $r = 3$ the fixpoint splits into two stable and one unstable branch, see Fig. 2.19, a typical bifurcation, as discussed in Sect. 2.2.

Bifurcation Cascade We may now carry out a stability analysis for $x_\pm^{(2)}$, just as we did for $x^{(1)}$. We find a critical value $r_3 > r_2$ such that

$$x_\pm^{(2)}(r) \ \text{ stable} \quad \Longleftrightarrow \quad \boxed{r_2 < r < r_3.} \tag{2.49}$$

Going further on one finds an r_4 such that there are four fixpoints of period 4, that is of $g(g(g(g(x))))$, for $r_3 < r < r_4$. In general there are critical values r_n and r_{n+1} such that there are

$$2^{n-1} \ \text{ fixpoints } x^{(n)} \text{ of period } 2^{n-1} \quad \Longleftrightarrow \quad \boxed{r_n < r < r_{n+1}.}$$

The logistic map therefore shows iterated bifurcations. This, however, is not yet chaotic behavior.

Chaos in the Logistic Map The critical r_n for doubling of the period converge:

$$\lim_{n\to\infty} r_n \;\to\; r_\infty, \qquad r_\infty = 3.5699456\ldots$$

There are consequently no stable fixpoints of $g(x)$ or of the iterated logistic map in the region

$$r_\infty \;<\; r \;<\; 4\,.$$

In order to characterize the sensitivity of Eq. (2.43) with respect to the initial condition, we consider two slightly different starting points x_1 and x_1':

$$x_1 - \; x_1' = y_1, \qquad |y_1| \;\ll\; 1\,.$$

The key question is then whether the difference

$$y_m = x_m - \; x_m', \qquad y_{m+1} \approx \frac{dg(x)}{dx}\Big|_{x=x_m} y_m \tag{2.50}$$

between the two respective orbits is still small after m iterations. For (2.50) we used $x_m' = x_m - y_m$, neglecting terms $\sim y_m^2$. We hence obtain

$$y_{m+1} = r(1-2x_m)\, y_m \equiv \epsilon\, y_m\,.$$

For $|\epsilon| < 1$ the map is stable, as two initially different populations close in with time passing. For $|\epsilon| > 1$ they diverge; the map is chaotic.

Lyapunov Exponents We remind ourselves of the definition

$$|\epsilon| = \mathrm{e}^{\lambda}, \qquad \lambda = \log\left|\frac{dg(x)}{dx}\right| \tag{2.51}$$

the Lyapunov exponent $\lambda = \lambda(r)$ of a map, as introduced in Sect. 2.2. For positive Lyapunov exponents the time development is exponentially sensitive to the initial conditions and shows chaotic features,

$$\lambda < 0 \;\Leftrightarrow\; \text{stability}, \qquad \lambda > 0 \;\Leftrightarrow\; \text{instability}\,.$$

This is indeed observed in nature, e.g. for populations of reindeer on isolated islands, as well as for the logistic map for $r_\infty < r < 4$, compare Fig. 2.19.

Maximal Lyapunov Exponent The Lyapunov exponent, as defined by Eq. (2.51) provides a description of the short time behavior. For a corresponding characterization of the long time dynamics one defines the "maximal Lyapunov exponent"

$$\lambda^{(max)} = \lim_{n\gg 1} \frac{1}{n} \log\left|\frac{dg^{(n)}(x)}{dx}\right|, \qquad g^{(n)}(x) = g(g^{(n-1)}(x))\,. \tag{2.52}$$

Using Eq. (2.51) for the short time evolution we can decompose $\lambda^{(max)}$ into an averaged sum of short time Lyapunov exponents. $\lambda^{(max)}$ is also denoted the "global Lyapunov exponent".

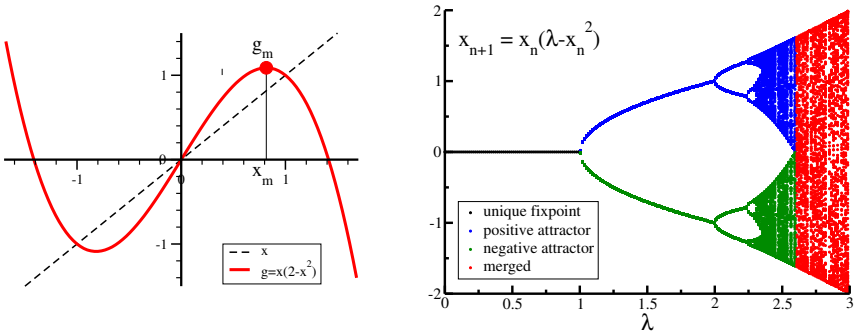

Fig. 2.20 **Left:** For $\lambda = 2$, the odd logistic map (2.53). The local maximum g_m is reached for $x_m = \sqrt{\lambda/3} \approx 0.82$. **Right:** The bifurcation diagram of the odd logistic map as a function of λ. One has a unique fixpoint $x_n = 0$ (black) for $\lambda < 1$ and two equivalent attractors (blue/green) for $1 < \lambda < \lambda_s$, which merge at $\lambda_s = \sqrt{27}/2 \approx 2.6$. Inversion symmetry is restored at λ_s (red). A period-doubling transition to chaos is observable in the symmetry broken phase.

One needs to select advisedly the number of iterations n in Eq. (2.52). On one side n should be large enough such that short-term fluctuations of the Lyapunov exponent are averaged out. The available phase space is however generically finite, for the logistic map $y \in [0, 1]$, and two initially close orbits cannot diverge ad infinitum. One needs hence to avoid phase-space restrictions, evaluating $\lambda^{(max)}$ for large but finite numbers of iterations n.

Routes to Chaos The chaotic regime $r_\infty < r < 4$ of the logistic map connects to the regular regime $0 < r < r_\infty$ with increasing period doubling. One speaks of a "route to chaos via period-doubling". The study of chaotic systems is a wide field of research and a series of routes leading from regular to chaotic behavior have been found. Two important alternative routes to chaos are:

- Intermittency route to chaos.
  The trajectories are almost periodic; they are interdispersed with regimes of irregular behaviour. The occurrence of these irregular bursts increases until the system becomes irregular.
- Ruelle–Takens–Newhouse route to chaos.
  A strange attractor appears in a dissipative system after two (Hopf) bifurcations. As a function of an external parameter a fixpoint evolves into a limit cycle (Hopf bifurcation), which then turns into a limiting torus, which subsequently turns into a strange attractor.

2.4.1 Colliding attractors

Bifurcations are generically the result of colliding invariant manifolds, viz of stable and unstable fixpoints, limit cycles and chaotic sets. Examples are the saddle-node bifurcation (2.19), at which a stable and an unstable fixpoint merge, and the collision between a limit cycle and a saddle within the Taken-Bogdanov system (2.33).

Odd Logistic Map The collision between two chaotic attractors can be studied within the odd logistic map

$$x_{n+1} = g(x_n) = x_n\big(\lambda - x_n^2\big), \qquad \lambda > 0\,, \tag{2.53}$$

which is invariant under inversion $x \leftrightarrow (-x)$. The local maximum $g_m = g(x_m)$ is given by

$$g' = 0, \qquad x_m = \sqrt{\frac{\lambda}{3}}, \qquad g_m = 2\sqrt{\frac{\lambda^3}{3^3}}\,, \tag{2.54}$$

as illustrated in Fig. 2.20.

Merging Chaotic Attranctors For $\lambda < 1$ only the trivial fixpoint exists. Afterwards, for $1 < \lambda < \lambda_s$, there are two attracting states that are related via inversion symmetry, as shown in Fig. 2.20. Both branches undergo a period-double transition to chaos, in equivalence to the one observed for the standard logistic map, compare Fig. 2.19. At λ_s, determined by

$$g(g_m) = 0, \qquad \lambda_s = 4\,\frac{\lambda_s^3}{3^3}, \qquad \lambda_s = \frac{\sqrt{27}}{2}\,, \tag{2.55}$$

the two attractors merge. Only a single chaotic attractor remains for $\lambda > \lambda_s$.

Chaotic Attractors in Crisis In general, different types of attractors may collide. A Hopf bifurcation, f.i., occurs when limit cycles contract to a point, which is equivalent to the merger of limit cycles with fixpoints. One speaks of a "crisis" when chaotic attractors collide with unstable fixpoints or limit cycles. For the logistic map (2.43) a crisis occurs at $r = 4$, namely when the chaotic attractor hits the unstable fixpoint $x = 0$. Orbits diverge for $r > 4$.

2.5 Dynamical Systems with Time Delays

The dynamical systems we have considered so far all had instantaneous dynamics, being of the type

$$\begin{aligned} \frac{d}{dt}y(t) &= f(y(t)), \qquad t > 0 \\ y(t=0) &= y_0\ , \end{aligned} \tag{2.56}$$

when denoting with y_0 the initial condition. This is the simplest case: one dimensional (a single dynamical variable only), autonomous ($f(y)$ is not an explicit function of time) and deterministic (no noise).

Time Delays In many real-world applications the couplings between different sub-systems and dynamical variables is not instantaneous. Signals and physical interactions need a certain time to travel from one subsystem to the next. Time delays are therefore encountered commonly and become important when the delay time T becomes comparable with the intrinsic time scales of the dynamical system. We consider here the simplest case, a noise-free one-dimensional dynamical system with a single delay time,

$$\begin{aligned} \frac{d}{dt}y(t) &= f(y(t), y(t-T)), \qquad t > 0 \\ y(t) &= \phi(t), \qquad\qquad\quad t \in [-T, 0] \ . \end{aligned} \tag{2.57}$$

Due to the delayed coupling we need now to specify an entire initial function $\phi(t)$. Differential equations containing one or more time delays need to be considered very carefully, with the time delay introducing an additional dimension to the problem. We will discuss here a few illustrative examples.

Linear Couplings We start with the linear differential equation

$$\frac{d}{dt}y(t) = -ay(t) \ - \ by(t-T), \qquad a, b > 0 \ . \tag{2.58}$$

The only constant solution for $a + b \neq 0$ is the trivial state $y(t) \equiv 0$. The trivial solution is stable in the absence of time delays, $T = 0$, whenever $a + b > 0$. The question is now, whether a finite T may change this.

We may expect the existence of a certain critical T_c, such that $y(t) \equiv 0$ remains stable for small time delays $0 \leq T < T_c$. In this case the initial function $\phi(t)$ will affect the orbit only transiently, in the long run the motion would be damped out, approaching the trivial state asymptotically for $t \to \infty$.

Hopf Bifurcation Trying our luck with the usual exponential ansatz, we find

$$\lambda = -a - b\mathrm{e}^{-\lambda T}, \qquad y(t) = y_0\mathrm{e}^{\lambda t}, \qquad \lambda = p + iq \ . \tag{2.59}$$

Separating into a real and an imaginary part we obtain

$$\begin{aligned} p + a &= -b\mathrm{e}^{-pT}\cos(qT), \\ q &= \ \ b\mathrm{e}^{-pT}\sin(qT). \end{aligned} \tag{2.60}$$

For $T = 0$ the solution is $p = -(a + b)$, $q = 0$, as expected, and the trivial solution $y(t) \equiv 0$ is stable. A numerical solution is shown in Fig. 2.21 for $a = 0.1$ and $b = 1$. The crossing point $p = 0$ is determined by

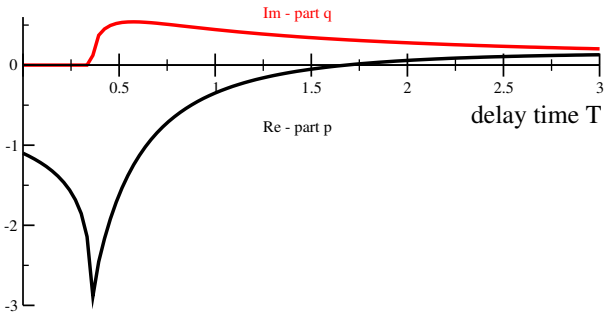

Fig. 2.21 The components p and q for the solution $e^{(p+iq)t}$, see (2.59), of the time-delayed system given by (2.58), for $a = 0.1$ and $b = 1$. The state $y(t) \equiv 0$ become unstable whenever the real part p becomes positive. The imaginary part q is given in units of π.

$$a = -b\cos(qT), \qquad q = b\sin(qT)\ . \tag{2.61}$$

The first condition in Eq. (2.61) can be satisfied only for $a < b$. Taking the squares in Eq. (2.61) and eliminating qT one has

$$q = \sqrt{b^2 - a^2}, \qquad T \equiv T_c = \arccos(-a/b)/q\ .$$

One therefore has a Hopf bifurcation at $T = T_c$ and the trivial solution becomes unstable for $T > T_c$. For the case $a = 0$ one has simply $q = b$, $T_c = \pi/(2b)$. Note, that there is a Hopf bifurcation only for $a < b$, viz whenever the time-delay dominates, and that q becomes non-zero well before the bifurcation point, compare Fig. 2.21. One has therefore a region of damped oscillatory behavior with $q \neq 0$ and $p < 0$.

Discontinuities For time-delayed differential equations one may specify an arbitrary initial function $\phi(t)$ and the solutions may in general show discontinuities in their derivatives, as a consequence. As an example we consider the case $a = 0$, $b = 1$ of Eq. (2.58), with a non-zero constant initial function,

$$\frac{d}{dt}y(t) = -y(t-T), \qquad \phi(t) \equiv 1\ . \tag{2.62}$$

The solution can be evaluated simply by stepwise integration,

$$y(t) - y(0) = \int_0^t dt'\dot{y}(t') = -\int_0^t dt' y(t'-T) = -\int_0^t dt' = -t,\ 0 < t < T\ .$$

The first derivative in consequently discontinuous at $t = 0$,

$$\lim_{t\to 0-}\frac{d}{dt}y(t) = 0, \qquad \lim_{t\to 0+}\frac{d}{dt}y(t) = -1\ .$$

For larger times, $T < t < 2T$, one finds

$$y(t) - y(T) = -\int_T^t dt' y(t'-T) = \int_T^t dt' \big[T - t'\big]$$
$$= T(t-T) - \frac{1}{2}\big(t^2 - T^2\big) = -\frac{1}{2}\big(T-t\big)^2,$$

and the second derivative has a discontinuity at $t = T$.

Dependence on Initial Function The solution of ordinary differential equations is determined by their initial condition and different initial conditions lead to distinct trajectories (injectivity). This is not necessarily the case anymore in the presence of time delays. We consider

$$\frac{d}{dt}y(t) = y(t-T)\big(y(t)-1\big), \qquad \phi(t=0) = 1\ . \tag{2.63}$$

For any $\phi(t)$ with $\phi(0) = 1$ the solution is $y(t) \equiv 1$ for all $t \in [0, \infty]$.

Non-Constant Time Delays Things may become rather weird when the time delays are not constant anymore. Consider

$$\begin{aligned} \tfrac{d}{dt}y(t) &= y\big(t - |y(t)| - 1\big) + \tfrac{1}{2}, \qquad t > 0, \\ \phi(t) &= \begin{cases} 0 & -1 < t < 0 \\ 1 & t < -1 \end{cases} . \end{aligned} \tag{2.64}$$

It is easy to see, that both functions

$$y(t) = \frac{t}{2}, \qquad y(t) = \frac{3t}{2}, \qquad t \in [0, 2]\ ,$$

are solutions of Eq. (2.64), with appropriate continuations for $t > 2$. Two different solutions of the same differential equation and identical initial conditions, this cannot happen for ordinary differential equations. It is evident, that special care must be taken when examining dynamical systems with time delays numerically.

2.5.1 Distributed time delays

Basic delay differential systems contain a single time delay T, like (2.58), which corresponds to an instanteous memory process. In general, the memory $y_M(t)$ of the past trajectory will be a convolution,

$$y_M(t) = \int_0^\infty K(\tau) y(t-\tau) d\tau, \qquad \int_0^\infty K(\tau) d\tau = 1\,, \tag{2.65}$$

where we defined with $K(\tau)$ the delay kernel. For a sharply peaked delay kernel, $K(\tau) = \delta(\tau - T)$, one recovers $y_M(t) = y(t-T)$.

Exponentially distributed time delays Explicitly we consider with

$$K(\tau) = \frac{1}{T}\,\mathrm{e}^{-\tau/T} \tag{2.66}$$

exponentially distributed time delays. One has

$$\frac{d}{dt}y_M(t) = \int_0^\infty d\tau K(\tau)\frac{d}{dt}y(t-\tau) = -\int_0^\infty d\tau K(\tau)\frac{d}{d\tau}y(t-\tau), \tag{2.67}$$

which allows to integrate the last expression by parts when using (2.66). The resulting closed expression,

$$\dot{y}_M = \frac{-1}{T}\int_0^\infty d\tau \mathrm{e}^{-\tau/T}\frac{d}{d\tau}y(t-\tau) = \frac{y-y_M}{T}\,, \tag{2.68}$$

corresponds to a trailing average, with the memory variable y_M trying to approach y.

Kernel series framework Eq. (2.68) implies that a delay differential equation with exponentially distributed delays can be mapped exactly to a system of ordinary differential equations by adding an additional variable, namely $x_m(t)$. For generic kernels $K(\tau)$ in (2.65) one can generalize this concept by adding a diverging number of memory variables. With this approach, denoted "kernel series framework", one can map any time delay system to a N-dimensional system of ordinary differential equations. For the case of a single time delay one speaks of the "linear chain trick". In general one has $N \to \infty$, which reflects the notion that delay stystems are formaly infinite dimensional.